Geophys. J. Int. (1996) **125**, 519–536

Reflection seismic investigations in the volcaniclastic apron of Gran Canaria and implications for its volcanic evolution

Thomas Funck,[1] Thomas Dickmann,[1] Roland Rihm,[1]
Sebastian Krastel,[1] Holger Lykke-Andersen[2] and Hans-Ulrich Schmincke[1]

[1]*Geomar Research Center for Marine Geosciences, Kiel University, Wischhofstrasse 1–3, 24148 Kiel, Germany*

[2]*Department of Earth Sciences, University of Aarhus, Finlandsgade 8, 8200 Aarhus N, Denmark*

Accepted 1995 December 19. Received 1995 September 19; in original form 1995 March 21

SUMMARY

High-resolution reflection seismic data obtained around Gran Canaria allow a detailed and consistent correlation of seismic reflectors of the northern and southern Canary Basins with the lithology drilled by DSDP Leg 47A SSE of Gran Canaria, as well as with major phases of volcanic activity on Gran Canaria as mapped onshore. Two prominent reflectors were chosen as marker horizons and correlated with the drilled lithology. The results indicate that reflector R7 above the Miocene volcaniclastic debris flows V1–V3 reflects the shield-building phase of Gran Canaria. Reflector R3 is interpreted as corresponding with the Pliocene Roque Nublo formation.

The top of the massive island flank of Gran Canaria, defined by seismically chaotic facies, extends 44 to 72 km off the coast of Gran Canaria. West of Gran Canaria the flank of Tenerife onlaps the steeper and older flank of Gran Canaria, which, in turn, is onlapping the older flank of Fuerteventura to the east in a similar way.

Erosional channels, which can also be traced up to 50 km from the area between Gran Canaria and Fuerteventura into the deeper northern basin, have been identified in the bathymetry.

The data presented provide new detailed information for modelling the submarine and subaerial evolution of the central Canary Islands of Gran Canaria and Tenerife, i.e. the timing of their shield-building phases and later stages of major volcanic activity, as reflected by the position of prominent seismic reflectors in the seismic stratigraphy.

Key words: Canary Islands, seismic reflection, volcanic activity.

INTRODUCTION

Present-day volcanic islands and seamounts are surrounded by large volcaniclastic aprons (Menard 1956), many of which exceed the volume of the entire edifice of the seamount or island from which they are derived through volcanic activity and erosion. They harbour a great wealth of material providing information on the temporal, bathymetric and compositional evolution of the magmatic source area. The submarine and subaerial growth and destruction of the source area, i.e. seamount or island (Fig. 1), is reflected in the volcaniclastic apron, which holds a long-term record of the ocean-island evolution.

A group of islands, rising several thousands of metres from the sea-floor and having basal diameters of 50 to 100 km, forms major morphological barriers to currents along and down the continental slope and can thus exert a strong influence on sedimentation patterns and evolution of sedimentary basins prior to and after growth of major volcanic barriers. The growth of the Canary Islands, where volcanism has progressed from east to west, may have led to massive erosion along the northwest African continental slope, documented by a large gap of about 1300 m in the sedimentary sequence drilled in DSDP Site 397A, equivalent to a major hiatus of about 100 Ma (Arthur *et al.* 1979). On the other hand, the influx of volcanic detritus generated by volcanic, hydroclastic, and epiclastic processes on the islands into the non-volcanic continent-derived sediments forms a significant part of the sedimentary columns to distances up to 1000 km away from an island.

The reconstruction of the evolution of Gran Canaria and Tenerife, as deduced from the study of products exposed on land (Schmincke 1982), can, by correlation of prominent seismic marker horizons, be extended over the entire sedimentation area surveyed during the recent research cruises M16 (Wefer *et al.* 1992) and M24 (Schmincke & Rihm 1994).

This paper deals mainly with the results of the high-resolution multi-channel reflection seismic data of 2117 km

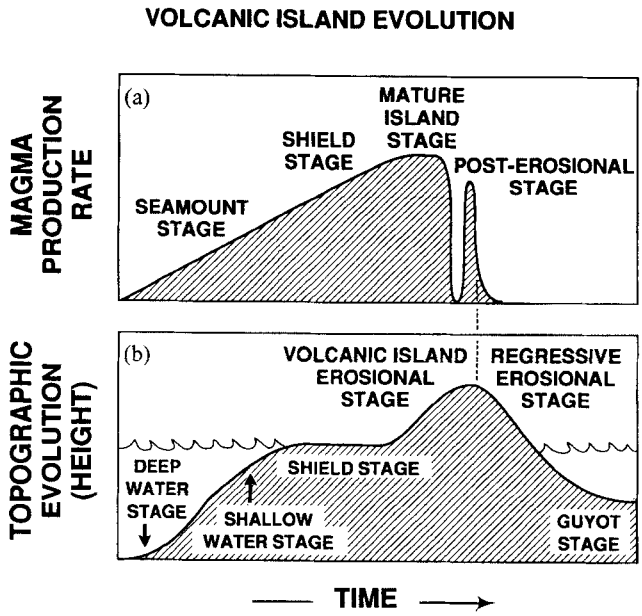

Figure 1. General scheme of temporal volcanic-island evolution (magma production rate and topography). Modified from Schmincke & Rihm (1994).

total length, which were obtained as a result of cooperation between Geomar Research Center, Kiel, and the Department of Earth Sciences of Aarhus University in 1993 during cruise M24 around Gran Canaria. This pre-site survey was followed by drilling into the volcaniclastic apron of Gran Canaria during ODP Leg 157 (ODP Leg 157 Shipboard Scientific Party 1995).

STRUCTURE OF OCEANIC VOLCANOES

Oceanic volcanoes consist of (1) a subaerial part, whose volume is generally less than 5 per cent and rarely exceeds 10 per cent of the total volume, and (2) a submarine part with an intrusive core and submarine extrusive rocks. They are surrounded by a volcaniclastic apron that, in a general volcanological and sedimentological sense, includes the volcanic debris and non-volcanic background sediments in the sedimentary basins adjacent to the volcanic edifice. The apron is increasingly well stratified with distance away from the island and may be traced sedimentologically for >1000 km. The volcanic debris that the volcanic aprons contain may equal or exceed the volume of the volcano, and the volcanic aprons contain significant amounts of material representing the evolution of the volcanic complex, including material no longer present on the island and material from unexposed and inaccessible submarine stages (Schmincke 1994).

The subaerial part of an oceanic volcano can be subdivided into a central core and the subaerial flanks or platforms. The submarine flanks comprise (1) a volcaniclastic top layer that separates the subaerial cap from (2) the deeper, mainly crystalline part of a submarine volcano, erupted non-explosively, and (3) a flank cover consisting of sediments, breccias, tephra, slump blocks and local lava flows. The submarine part is composed largely of pillow lavas, densely packed and non-vesicular at depth, but becoming increasingly vesicular and interlayered with pillow breccias and pillow fragment breccias and primary and resedimented hyaloclastites upwards.

The hyaloclastic upper extrusive section is overlain by volcaniclastic debris flows which contain abundant tachylite and a wide variety of subaerial volcanic and subvolcanic rock fragments (ranging from microgabbro to trachyte), dominated by alkali basalt.

VOLCANIC EVOLUTION OF GRAN CANARIA

Gran Canaria (28° 00'N, 15° 35'W) is the central island of the volcanic Canarian archipelago in the central eastern Atlantic, some 100 km off the north-western African passive continental margin. It is one of the best-studied oceanic islands with respect to stratigraphy, volcanology, geochemistry and geochronology. All subaerially exposed volcanic and intrusive rocks were formed within the last 16 Ma (McDougall & Schmincke 1976).

Three major subaerial magmatic/volcanic cycles have been distinguished on Gran Canaria (Fig. 2), which have been further subdivided into several stages (Schmincke 1976, 1982, 1994; Hoernle, Tilton & Schmincke 1991; Hoernle & Schmincke 1993a, b).

(1) The Miocene cycle started with the rapid formation (*ca.* 1 Ma) of the subaerial volcanic shield. At 14 Ma, the basaltic shield phase was followed by 0.5 Ma long volcanism of trachytic to rhyolitic composition (forming approximately 15 major ignimbrite cooling units), generating what is by far the largest volume of silicic volcanic rocks on any oceanic intraplate volcanic island. After the rhyolitic stage, about 500 km^3 of silica-undersaturated nepheline trachyphonolitic ash flows, lava flows and fallout tephra and rare basanite and nephelinite dykes and lavas were erupted between 13 and *ca.* 9.5 Ma.

(2) Following a major non-volcanic hiatus lasting approximately 4–5 Ma, the Pliocene cycle began at *ca.* 5 Ma (Fig. 2), with lavas becoming systematically more SiO_2-saturated. Peak activity occurred at around 4 Ma (Roque Nublo group). After a possible brief hiatus, there was a resurgence in volcanism, during which only highly undersaturated mafic volcanics were erupted (3.2–1.7 Ma).

(3) During the Quaternary, volcanism was restricted almost exclusively to the northern half of the island. The island can be considered volcanically active, as testified by numerous prehistoric basanite scoria cones, maars and lava flows as young as 3000 yr BP.

Monitoring of the submarine development of the Canary Islands can be achieved by the study of volcaniclastic sediments encountered in drill holes, such as those of DSDP Site 397, 100 km SSE of Gran Canaria (von Rad *et al.* 1979), and the VICAP Sites around Gran Canaria drilled in 1994 during ODP Leg 157 (ODP Leg 157 Shipboard Scientific Party 1995). In Site 397, hyaloclastite debris flows are interpreted as representing material from the submarine stage of an island (probably Fuerteventura) transported for more than 100 km to the south and south-west (Schmincke & von Rad 1979). The overlying debris flows, which are rich in alkali basalt fragments, are interpreted as representing the shallow-water and shield stages of emerging Gran Canaria (Schmincke 1994). They form the bulk of the debris flows mapped seismically by

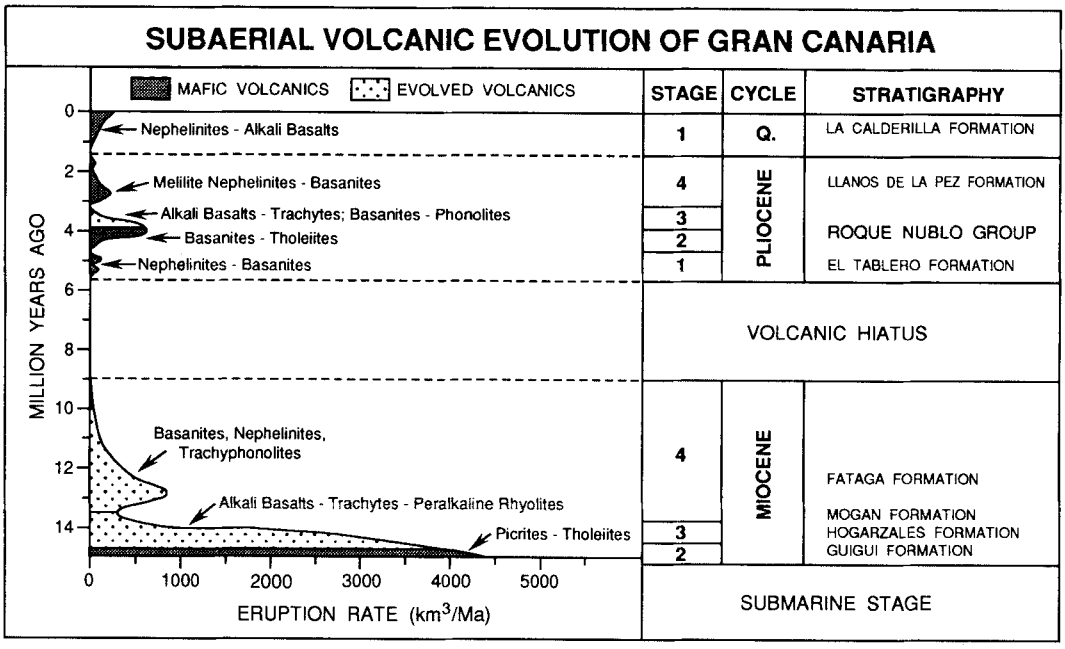

Figure 2. Subaerial evolution of Gran Canaria (volcanic cycles). Modified from Hoernle, Tilton & Schmincke (1991).

Wissmann (1979) and are thus thought to reflect the rapid growth of an island during the shield stage (Fig. 1). A very large amount of clastic debris is generated during the transition period seamount or island by phreatomagmatic and magmatic explosive activity, as well as by erosion of freshly formed pyroclastic deposits.

Younger ash layers of DSDP Sites 369 and 397 reflect later, differentiated, subaerial stages of an island, such as the 13 to 14 Ma old rhyolite ashes from Gran Canaria or the phonolitic Pliocene/Pleistocene ash layers, most of which are probably the result of Plinian eruptions on Tenerife (Rothe & Koch 1978; Schmincke & von Rad 1979). Such ash layers deposited from explosive eruptions on the islands provide excellent stratigraphic marker beds in the clastic aprons surrounding the islands and thus represent the most important tool for correlation of seismic stratigraphy with volcanic events.

PREVIOUS SEISMIC INVESTIGATIONS

Single- and multi-channel reflection seismic profiles from the continental margin off Western Africa and the Canary Islands (e.g. RV KANE; RV ATLANTIS cruises 1967, 1975; RV VALDIVIA 10; RV METEOR cruises 25 1971, 39 1975, 46 1978; DV GLOMAR CHALLENGER ship track profiles Leg 47 1976; Seibold & Hinz 1976; Uchupi *et al.* 1976; Wissmann 1979) have already shown flanks of highly reflective material surrounding the volcanic ocean islands and seamounts of the region, and thus demonstrated the strong influence of volcaniclastic material on the construction of the sedimentary sequences in the area.

During DV GLOMAR CHALLENGER Leg 47A, DSDP Site 397 was drilled with a total penetration of 1453 m (see Fig. 10). The most prominent reflector, R7, which had been thought to represent the Cretaceous–Tertiary boundary, was found to consist of several thick Miocene volcaniclastic debris- and mass-flow deposits (von Rad *et al.* 1979), which is also seismically confirmed by profile M46–37 (Wissmann 1979). Other prominent reflectors were established, by drilling, to be largely composed of volcaniclastic material, including reflector R3, which we use, together with reflector R7, as a marker horizon to reconstruct the sedimentary history around Gran Canaria.

A geophysical study of the volcaniclastic apron south-west of Gran Canaria, employing multi-channel reflection seismic (48 channels, 2.4 km), high-resolution multi-channel reflection seismic (6 channels, 80 m), gravity, magnetic, echosounding (Parasound) and swath bathymetric (Hydrosweep) recording on all profiles, and refraction seismic recording on two profiles (P1 + P11), was carried out during METEOR cruise M16–4, 1991 (Wefer *et al.* 1992). The profile orientation and spacing, with a total length of 950 km, were chosen in order to allow identification of the outer limit of the seismically defined chaotic facies, i.e. the extension of the submarine volcanic edifice. The profile locations are shown in Fig. 3. Results of this cruise are presented in Hirschleber *et al.* (1992), Geisslinger (1993) and Thywissen & Wong (1993).

THE METEOR 24 PROJECT

The goal of METEOR cruise M24 was a detailed survey of the north-eastern, northern and western parts of the volcaniclastic apron around the prototype oceanic volcanic island of Gran Canaria. Together with METEOR cruise M16, M24 served as the major pre-site survey for the VICAP drilling project. Hydrosweep and Parasound, seismic reflection and refraction, magnetic and gravity data were collected (see also Dañobeitia, Canales & Dehghani 1994). Additionally, a deep seismic study was carried out during cruise M24 using ocean-bottom seismometers in combination with land-based seismometers (Ye *et al.* 1995).

Data acquisition and processing

Reflection seismics

The seismic fieldwork of the M24 cruise was carried out as a cooperation between Geomar Research Center, Kiel, Germany

Table 1. Source and recording parameters.

Acoustic source	4 sleeve guns HGS (4×40 inch$^3 \approx 4 \times 0.66$ l)
Streamer	Teledyne–24 Channels Hydrophones per group 7 Group spacing 6.25 m Group length 3.125 m 143.75 m active length
Recording system	EG&G Geometrics ES2420 Sample interval 1 ms

and the Department of Earth Sciences, University of Aarhus, Denmark. The source and recording parameters of the 50 profiles (Fig. 3), with a total length of 2117 km, are summarized in Table 1.

The shot distances of 12.5 m, 18.75 m and 25 m were chosen according to water depths of <1125 m, 1125–3000 m and >3000 m, respectively. With these three shotpoint distances, a six-, four- and three-fold coverage was obtained. The first stage of onshore processing was carried out at the University of Aarhus, where all profiles were processed with a standard processing program (NORSEIS, GECO) to give stacked sections. An additional post-stack processing was accomplished at Geomar. The seismic frequency spectra lie in a bandwidth of

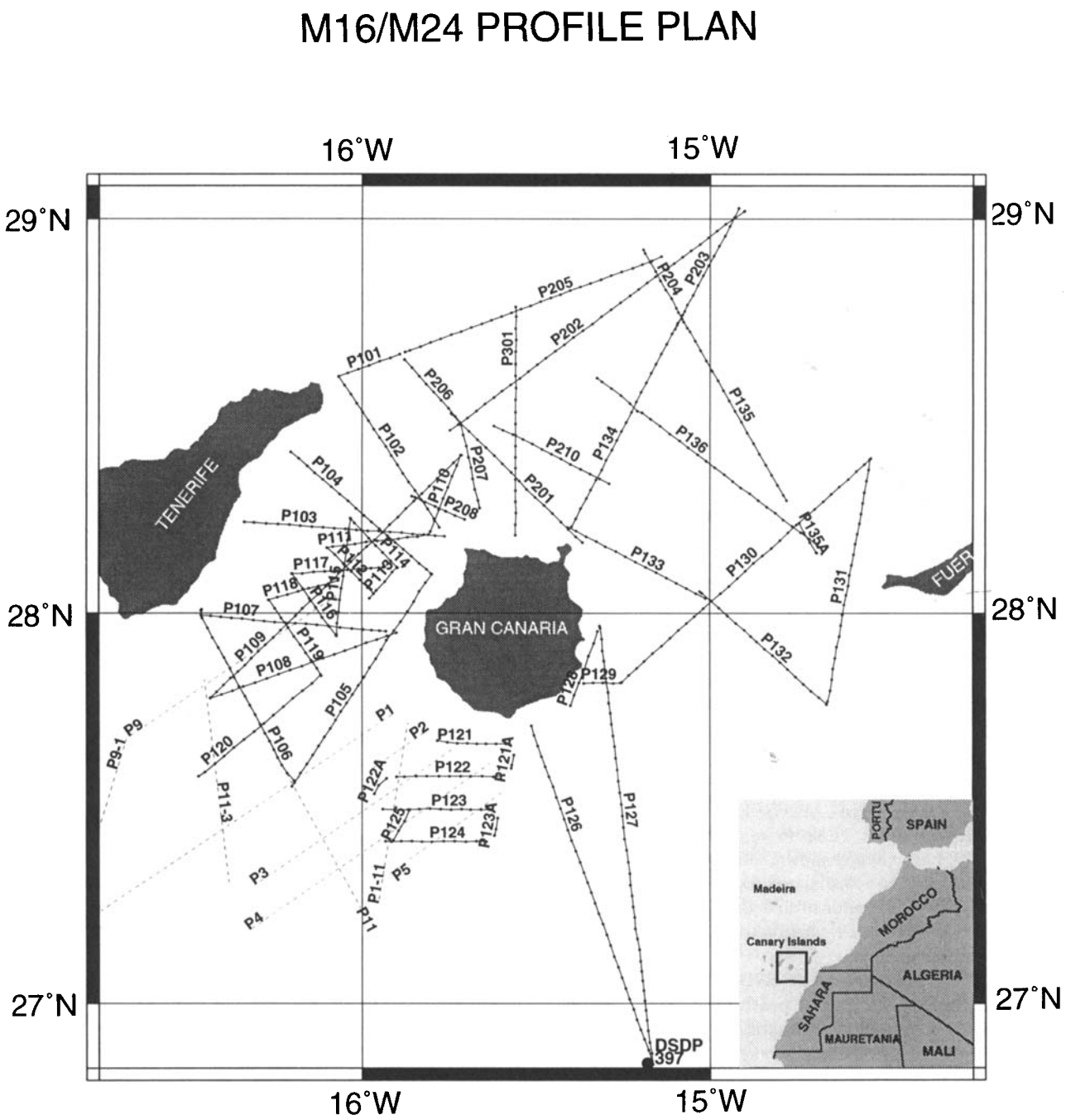

Figure 3. Profile plan of METEOR cruises 16 (dashed lines) and 24 (solid lines ticked at every 1000th CDP).

20 Hz to at most 240 Hz. An uncritical resampling from 1 to 2 ms sampling interval was carried out with regard to economic processing, particularly for the migration. Due to varying data quality, time-variant frequency filtering was mostly applied with a bandwidth from 30 to 220 Hz at the seafloor and to 70 Hz two seconds below the seafloor. Although the present CMP trace spacing is very dense (3.125 m), spatial aliasing was observed in cases where the diffraction tails dip very steeply. To avoid dispersive noise on the migrated sections, aliased energy needed to be filtered out with a high-cut frequency filter, or in some cases with a dip filter (fk-filter), to remove spatial aliased seismic energy.

Bearing in mind the problem of spatial aliasing, as for the migration, it was possible to generate stacked sections by summing four adjacent CMP stacked traces on the more-or-less horizontally layered sections far away from the steep volcanic flanks. This trace- and time-saving routine for the subsequent processes significantly enhanced the signal-to-noise ratio with no loss of resolution, resulting in a CMP trace spacing of 12.5 m in the corresponding areas.

The last step of standard data processing was migration, performed with the GEOSYS program at Geomar. Time migration was applied to the CMP stacked sections as an approximation to zero-offset sections in order to move dipping reflectors into their true subsurface positions and to collapse diffractions, resulting in a better spatial resolution for the interpretation. Such diffractions are very often observed in the M24 seismic-reflection data, especially at the steep island flanks. No intensive stacking velocity analysis was carried out in Aarhus due to the very short streamer of 150 m and the usually great water depth. The only way to obtain velocity information was a migration velocity analysis. For this analysis a time migration in the frequency–wavenumber (fk) domain was applied, assuming a homogeneous subsurface. A velocity model was constructed from this analysis of migration velocities at prominent horizons. For the final model a finite-difference migration was applied. The finite-difference method is very robust in tolerating large velocity errors. Its algorithm in the frequency–space (fx) domain, based on the 45° approximation to the scalar wave equation, is very effective for steep-dipping events, without introducing much dispersive noise. It was applied to the data sections of the steep island flanks. On the remaining data sections the faster finite-difference method in the time–space (tx) domain was applied in order to save computer time. After migration, a mute to the water layer was applied.

The depth penetration of the seismic energy strongly depends on sediment and rock types. The basalts of the submarine volcanic shield, which could not in general be penetrated by the pulses of our seismic system, act as an acoustic basement. Only below the feather edges of the island flanks, where the basalts are already noticeably thinned, do some weak and discontinuous reflections become visible. On most profiles in deep water, penetration reaches 600 to 2000 ms TWT, the variations depending, to a large extent, on the weather conditions during the cruise.

Multibeam bathymetry

The bathymetric mapping of the steep slopes of Gran Canaria and the more distant ocean floor was carried out using the Krupp Atlas Hydrosweep system. This survey echosounder provides wide-swath sweeps with a width equal to twice the water depth. The onshore processing of the Hydrosweep data collected during the cruises M16 and M24 was made on a SUN workstation using the mbsystem software developed at the Lamont-Doherty Earth Observatory. After computing new depth values using a water-velocity function representative for the survey area (databank mblevitus of the mbsystem), erroneous swaths and single beams (mostly the outer four) were removed. Gaps without any coverage of Hydrosweep data were filled with GEODAS data (National Geophysical Data Center 1993) and at a few locations with GEBCO data (British Oceanographic Data Centre 1994). Finally, the consistent data set was gridded using a grid of sufficient density (cell dimension 930 m E–W by 1010 m N–S) and applying a spline interpolation for data gaps.

The most detailed bathymetric chart available previously was a compilation by Hunter, Searle & Laughton (1980) at a scale of 1:2 000 000 at 41°N. Now we present a contour map compiled from the Hydrosweep data of METEOR cruises M16 and M24, which is shown in Fig. 4. This map represents a unique and essential tool for analysing erosional processes and the distribution, shape and size of primary volcanic features, as well as the evolution of submarine deltas and canyons.

DISCUSSION AND CONCLUSIONS

The submarine volcanic flanks

The most remarkable features in the reflection seismic lines around Gran Canaria are the submarine island flanks formed by the top of the massive volcanic edifices of Gran Canaria and the adjacent islands of Fuerteventura in the east and Tenerife in the west. In the unmigrated sections the steep slopes of the islands are characterized by numerous diffraction hyperbola caused by the rough morphology of the volcanic products. Many of these diffractions are of a 3-D nature, for example side echos, and could therefore not be condensed completely to their apex by the 2-D migration techniques applied. The dip of the slope of Gran Canaria is up to 25°–30° (e.g. profile 134, Fig. 5). Further off the island the dip of the flank decreases, while the thickness of the overlying sediments increases. The occurrence of diffraction hyperbola at the top of the flank becomes rare; the seismic facies of the volcanic shield is here characterized by a high-amplitude reflection with a discontinuous, mounded structure. In general the volcanic flank acts as the acoustic basement. Close to the feather edge, the top of the volcanic pedestal is gentle, almost horizontal, and sometimes short branches of underlying reflectors become visible. They are mostly horizontal and discontinuous. The weak seismic source and short receiver length restrict a better definition of the bottom of the volcanic edifice (question mark in Fig. 5).

It is possible to decipher details of the temporal succession of the submarine phases of the islands of Fuerteventura, Gran Canaria and Tenerife by analysing the records of their flanks. This kind of information is not available from the ages obtained for the subaerial parts of these islands (McDougall & Schmincke 1976; Schmincke 1982; Coello *et al.* 1992; Ancochea *et al.* 1990) because the submarine portions are not accessible onshore.

(1) It is evident that the most easterly island of

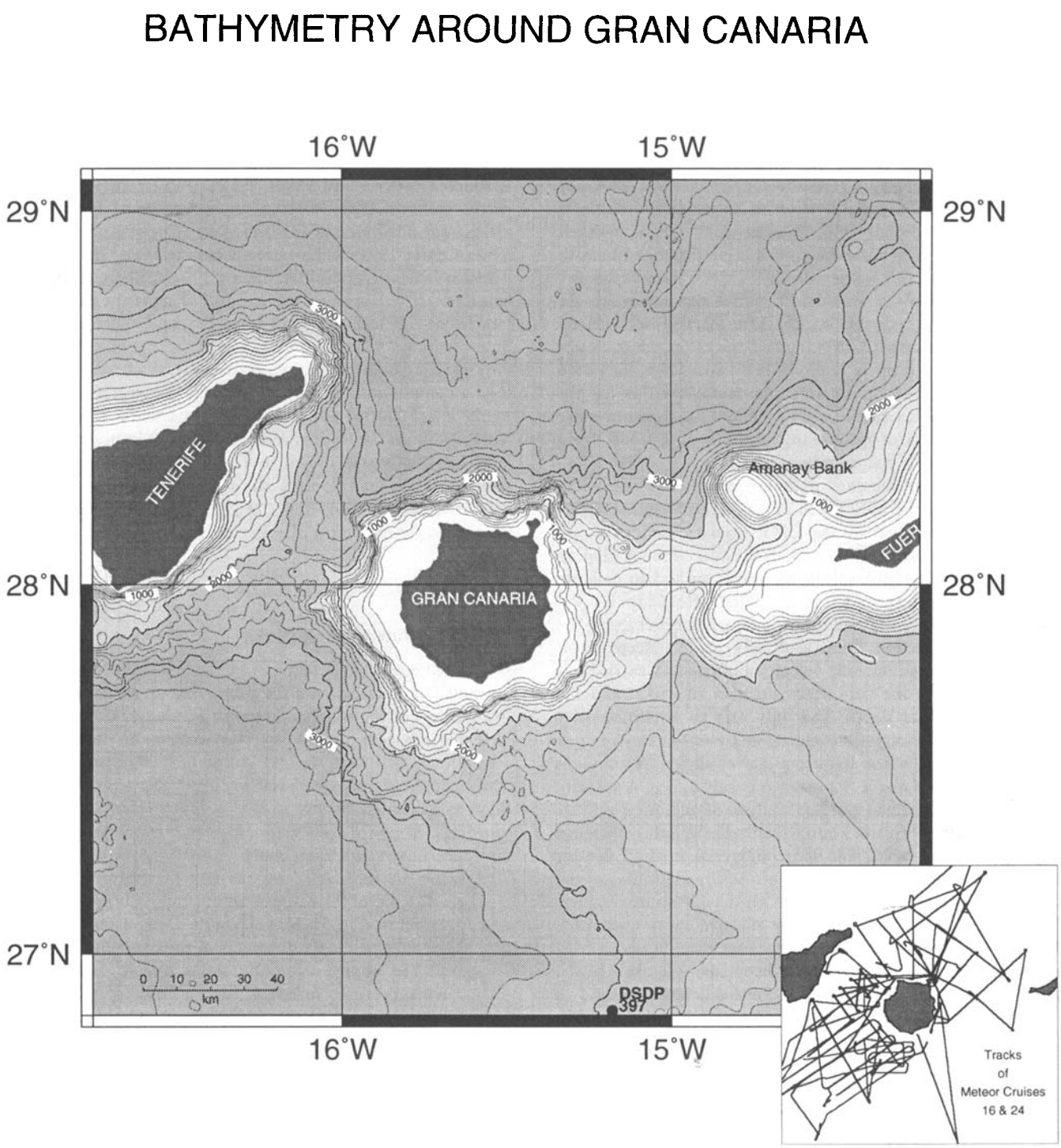

Figure 4. Bathymetric map of the research area (swath bathymetry of METEOR cruises M16 and M24, supplemented by GEODAS and GEBCO data). Contour interval 200 m.

Fuerteventura is older than Gran Canaria from correlation of the flank of the so-far unnamed (Ranke, von Rad & Wissmann 1982), roughly 60 m deep morphological guyot at 28°13′N, 14°46′W (which is connected with the volcanic edifice of Fuerteventura) on profile 135 and the flank of Gran Canaria. Since morphological guyots with a depth of less than 200 m are called banks (Menard 1964) and since the plateau is mentioned as Amanay Shallow in navigational charts, we suggest the name Amanay Bank for this volcanic feature. A comparison of the stratigraphic position of both feather edges of the flanks in the surrounding basin shows that Fuerteventura is approximately 180 ms TWT deeper than Gran Canaria (Gran Canaria on profile 134: 5660 ms TWT; Fuerteventura on profile 135: 5840 ms; see also Fig. 6). Since the submarine shield of Fuerteventura is older than that of Gran Canaria, deposition of volcanic material produced during the shield stage of Gran Canaria was limited by the adjacent shield of Fuerteventura. There was no room for an undisturbed distri-

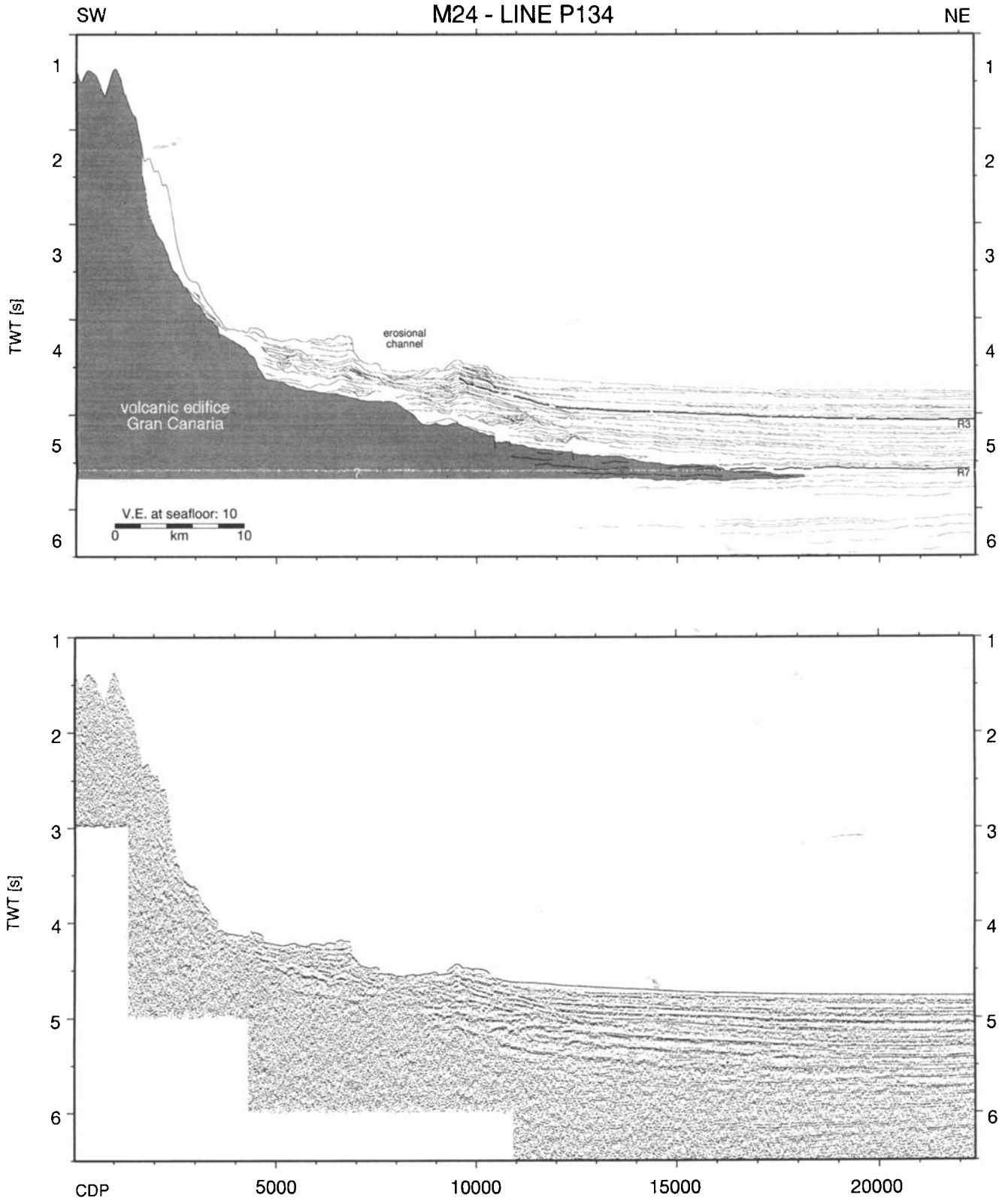

Figure 5. Time-migrated seismic line 134 and line drawing.

bution of the volcanic material, resulting in the observed ponding of the Gran Canaria shield against Fuerteventura (Fig. 6). In comparison with the other profiles, the eastern flank of Gran Canaria is relatively flat and onlaps the flank of Fuerteventura at a depth of only 2 km (2.7 s TWT), whereas its depth in the north (e.g. profile 134, Fig. 5) is 5.7 s TWT (approx. 4.5 km). The ponding is also indicated on the bathymetric maps (Figs 4 and 9), where flat relief east of Gran

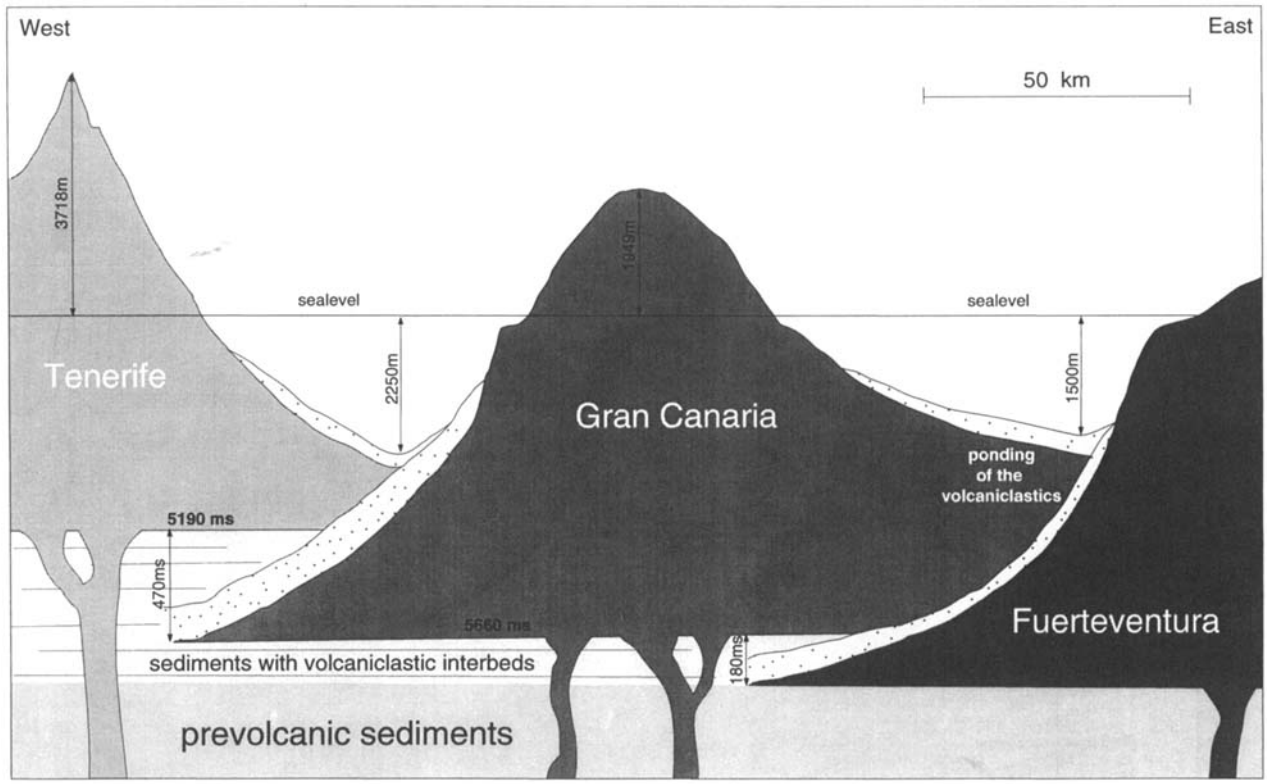

Figure 6. Schematic profile crossing Fuerteventura, Gran Canaria and Tenerife.

Canaria forms the 1550 m deep broad topographic swell between Gran Canaria and Fuerteventura.

(2) The submarine part of Gran Canaria is older than Tenerife. The onlap of the island flank of Tenerife on Gran Canaria is evident from profile 112 (Fig. 7), situated in the northern region of the channel between these two islands. The shield of Tenerife seems to be thin, i.e. transparent enough to allow correlation of energy reflected below it. The intercalation of the volcanic edifice of Tenerife with the well-stratified sedimentary basin north of Gran Canaria is shown in Fig. 8. The feather edge of the flank is located at a depth of 5190 ms TWT. By comparison of the stratigraphy in the northern basin with DSDP Site 397 (von Rad *et al.* 1979), the southern reflector, R3, can also be identified in the north (see below). Thus, an estimation of the age of the northern submarine shield of Tenerife is possible. On profile 205 (Fig. 8) the ratio of the TWT between the seafloor and the prominent reflector R3 to the TWT between the seafloor and the top of the flank of Tenerife is approximately 2:3. Assuming a constant sedimentation rate and an age of 3.8 Ma for the reflector R3, an age of roughly 6 Ma for the northern submarine part of Tenerife appears reasonable. This is in good agreement with data published by Ancochea *et al.* (1990), where the K-Ar determinations for the eastern part of the Anaga massif at the northeastern tip of Tenerife are around 5.7 Ma. The more-or-less contemporaneous ages for the subaerial parts of the Anaga massif and the submarine shield indicate rapid growth of the volcanic shield of Anaga.

The evolution of the central part of the channel between Gran Canaria and Tenerife resembles that between Fuerteventura and Gran Canaria. The older flank of Gran Canaria was deposited westwards into the 'open ocean', while the later growth of Tenerife to the east was hindered by the already existing island of Gran Canaria (Fig. 6). We interpret this as the reason why the eastern flank of Tenerife has a more gentle dip and onlaps the steeper flank of Gran Canaria.

In the southern part of the channel the ratio of the TWT of reflector R3 to the top of the flank of Tenerife (measured from the seafloor) is approximately 1:2 (profile 106), implying an age of some 8 Ma for this part of the volcanic edifice. Physical ages reported by Ancochea *et al.* (1990) for the basaltic series of Roque del Conde in the southern part of Tenerife are mainly between 8.5 and 6.4 Ma. In summary, the submarine portions of Tenerife are younger in the northeast than in the south, as are the corresponding subaerial parts.

Fig. 9 shows the extent of the submarine island flanks of Gran Canaria and the adjacent islands of Fuerteventura and Tenerife and their coverage by the seismic net. In the south-eastern region some additional profiles were used for mapping, which were collected during METEOR cruise M16 (Wefer *et al.* 1992) and processed by Geisslinger (1993). In both channels between the islands no information is available about the extent of the respectively older flank due to the limited penetration of the seismic energy in the rocks of the volcanic shield.

The massive island flank of Gran Canaria extends 44 to 72 km off the coast. East of Gran Canaria the flank terminates closest to the shore, where its growth was limited by the pre-existing volcanic shield of Fuerteventura. In the northern basin the flank extends some 60 km seawards; in the southern basin, between 54 and 72 km. Towards Tenerife, the flank of Tenerife is as close as 24 km to Gran Canaria. The extent of the flank of Tenerife varies between 30 and 40 km in the channel towards

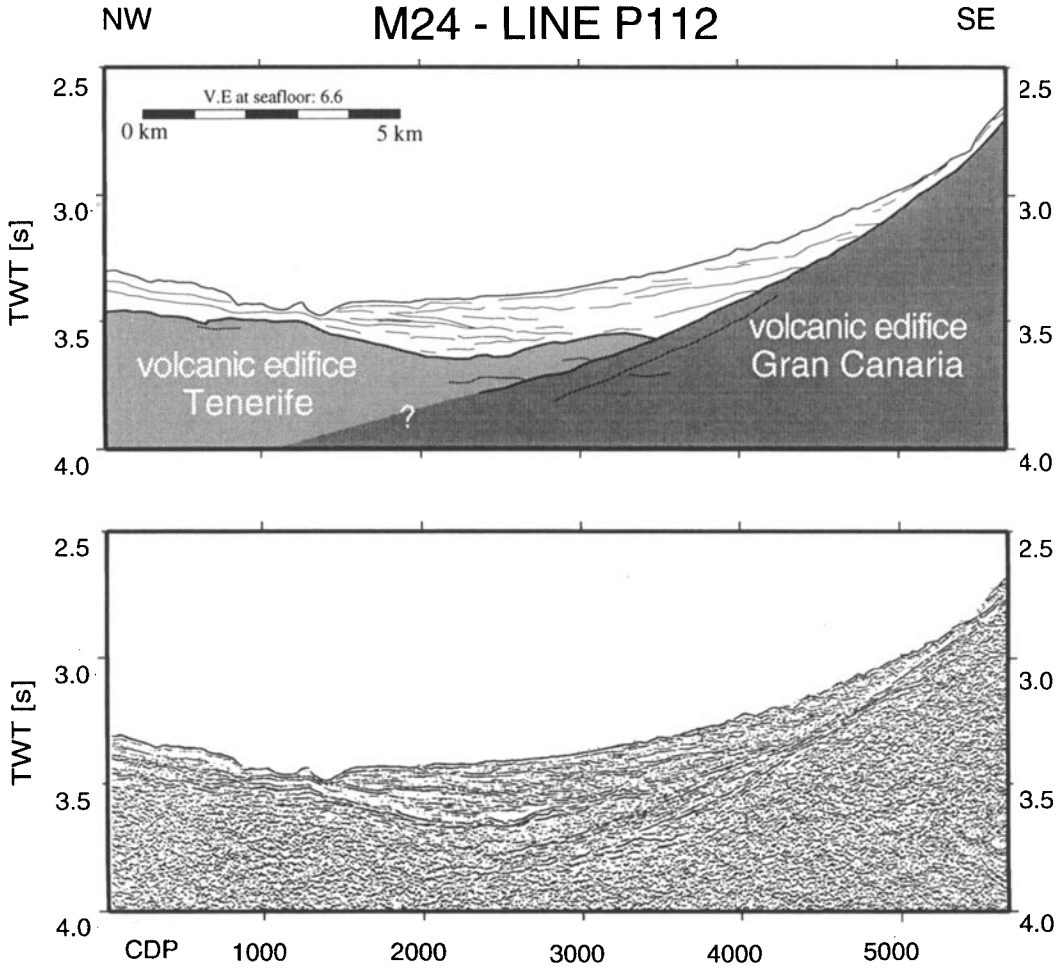

Figure 7. Time-migrated seismic line 112 and line drawing.

Gran Canaria, between 40 and 50 km in the southern region and around 50 km in the northeast.

Erosional features between the islands

It is not possible to correlate seismic reflectors continuously across the island channels from south to north because (1) many reflectors terminate and onlap at the volcanic flanks and (2) the main depositional processes in the proximal facies between the islands may have been mass-wasting events (debris flows and landslides), resulting in more-or-less chaotic reflection patterns. Source areas for these deposits are both of the islands adjacent to the channel, which complicates the interpretation.

None the less, there are some areas between the islands with stratified sedimentation filling local deeps of the uneven relief of the volcanic edifice (some indications of this are shown in Fig. 7). The reflection pattern in these areas is in general different from the basins due to local, smaller mass-wasting events from the adjacent islands. This factor, together with the isolated location of such sediment pockets, causes dating of the deposits to be hampered and mostly impossible.

The approximately 1550 m deep channel between Gran Canaria and Fuerteventura shows more distinct erosional features than the channel between Tenerife and Gran Canaria, which is 700 m deeper and younger by several million years (Fig. 4). The volcanic edifice between Gran Canaria and Fuerteventura has a rough topography with large depth variations of up to 750 m over a horizontal distance of less than 2 km. This relief seems to be caused by erosion, as indicated by several erosional channels that can be traced on the bathymetric map (Fig. 4). One prominent erosional channel crosses profile 134 (Fig. 5) between CDP 6900 and 9500, where some 200 m of sediments have been eroded. Further to the south, at the crossing with profile 133, only some debris (several tens of metres) is found in the channel, which itself cuts approximately 350 m deep into the volcanic edifice of Gran Canaria. This channel can be traced for more than 50 km, leading into the deep northern sediment basin.

Sedimentation in the apron

Several different types of seismic facies are found in the volcanic apron (Fig. 5). Close to the island the reflection patterns are mostly chaotic, representing mass-wasting processes downslope, with numerous terminations. Some isolated small basins within the volcanic edifice are filled with well-stratified sediments, especially in the channels between the islands. Further seaward the sedimentation becomes increasingly stratified, with parallel to subparallel reflectors at intermediate distances, and almost parallel reflectors in the deep basin. The

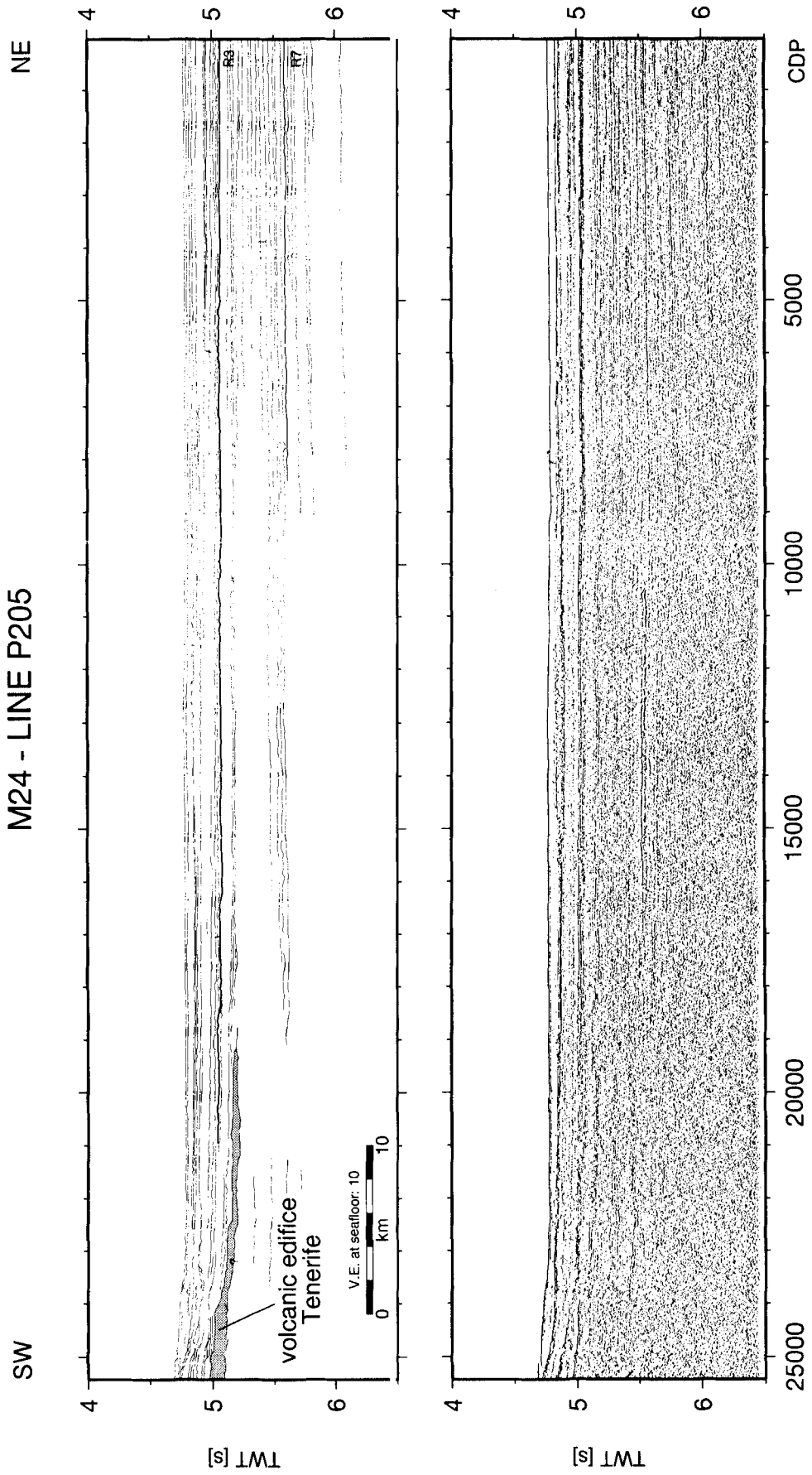

Figure 8. Time-migrated seismic line 205 and line drawing.

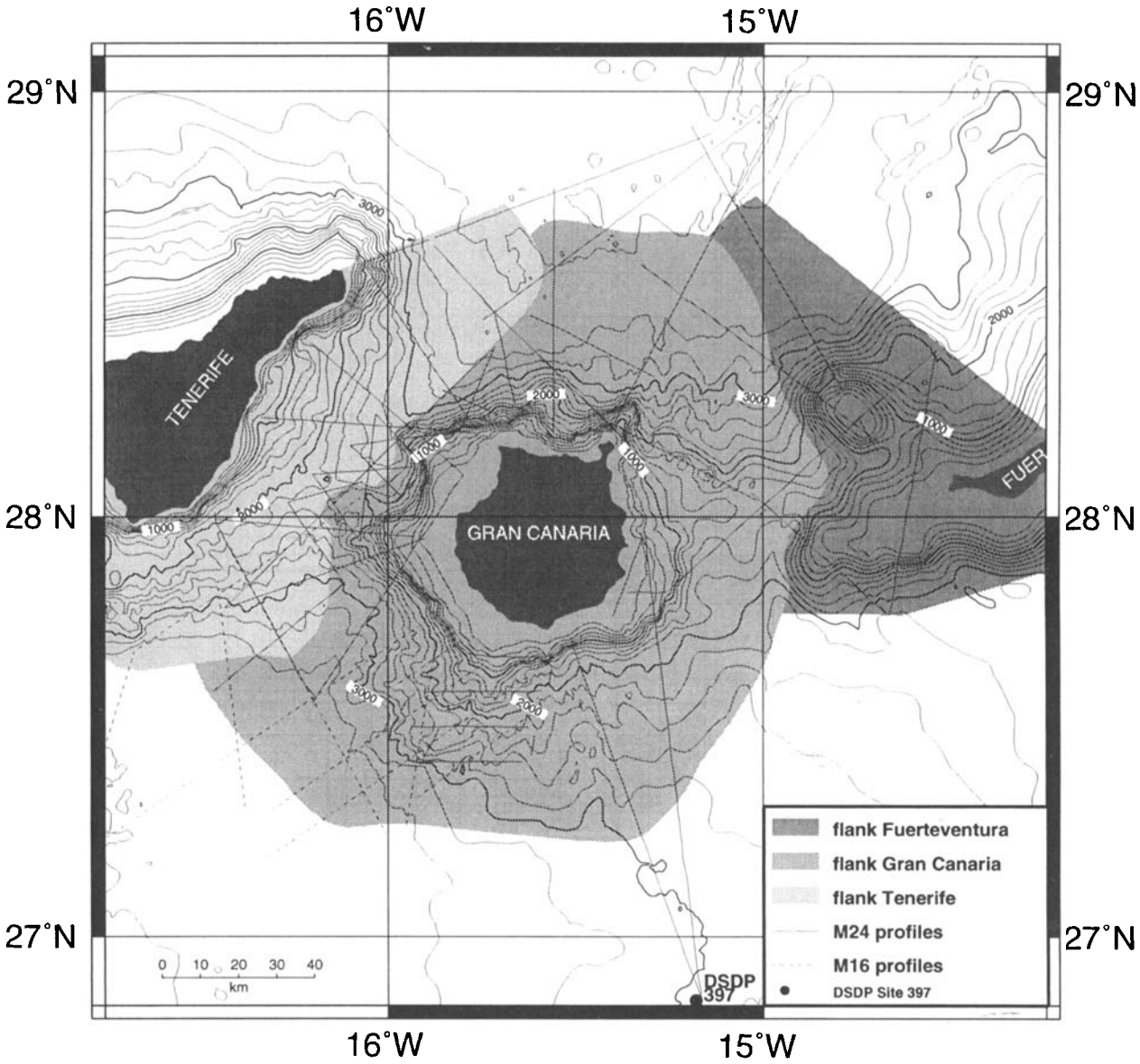

Figure 9. Extension of the submarine flanks of Fuerteventura, Gran Canaria and Tenerife, shown together with the bathymetry (contour interval 200 m).

number of terminations decreases with increasing distance from the island.

In general, the apron is characterized by numerous high-amplitude reflections with a high continuity, due to the high content of volcaniclastic material, which has a large impedance contrast compared to the surrounding hemipelagic background sedimentation. A large amount of volcaniclastic material is still present more than 100 km south-east of Gran Canaria at DSDP Site 397 (von Rad *et al.* 1979).

The two radial profiles, 126 and 127, in the southern basin pass approximately 1.4 km to the east of DSDP Site 397. A correlation with the reflectors found at the drill site is possible, even though the data quality of the two lines is comparatively poor due to heavy seas during data acquisition. Fig. 10 shows the reflectors R1 to R10, as identified during drilling (von Rad *et al.* 1979; Wissmann 1979) and their equivalents on profile 126. The deepest reflector, R10, could not be identified with certainty and hence is not labelled.

Two reflectors, R3 and R7, are described in more detail. At DSDP Site 397, R7 is bedded between an unconformity representing the hiatus from 12.5 to 10.5 Ma and the 16 to 17 Ma old volcaniclastic debris flows (Fig. 10). Based on magnetostratigraphy, R7 is itself approximately 13 Ma old. Correlation of R7 towards the flank of Gran Canaria shows it to onlap the flank as the oldest prominent reflector. This criterion was used to identify R7 in the northern basin of Gran Canaria, since direct correlation across the island channels was not possible, as already discussed.

According to magnetostratigraphy, the reflector R3 at DSDP Site 397 is approximately 4 Ma old, and biostratigraphy based on calcareous nanoplankton assigns R3 to zone NN14, corresponding to an age interval of 3.8 to 4.0 Ma (von Rad *et al.* 1979). R3 thus corresponds to the Pliocene Roque Nublo phase of volcanism on Gran Canaria. R3 is characterized by a significant high-amplitude reflection band. Similar reflection patterns are found south-east and north of Gran Canaria. The

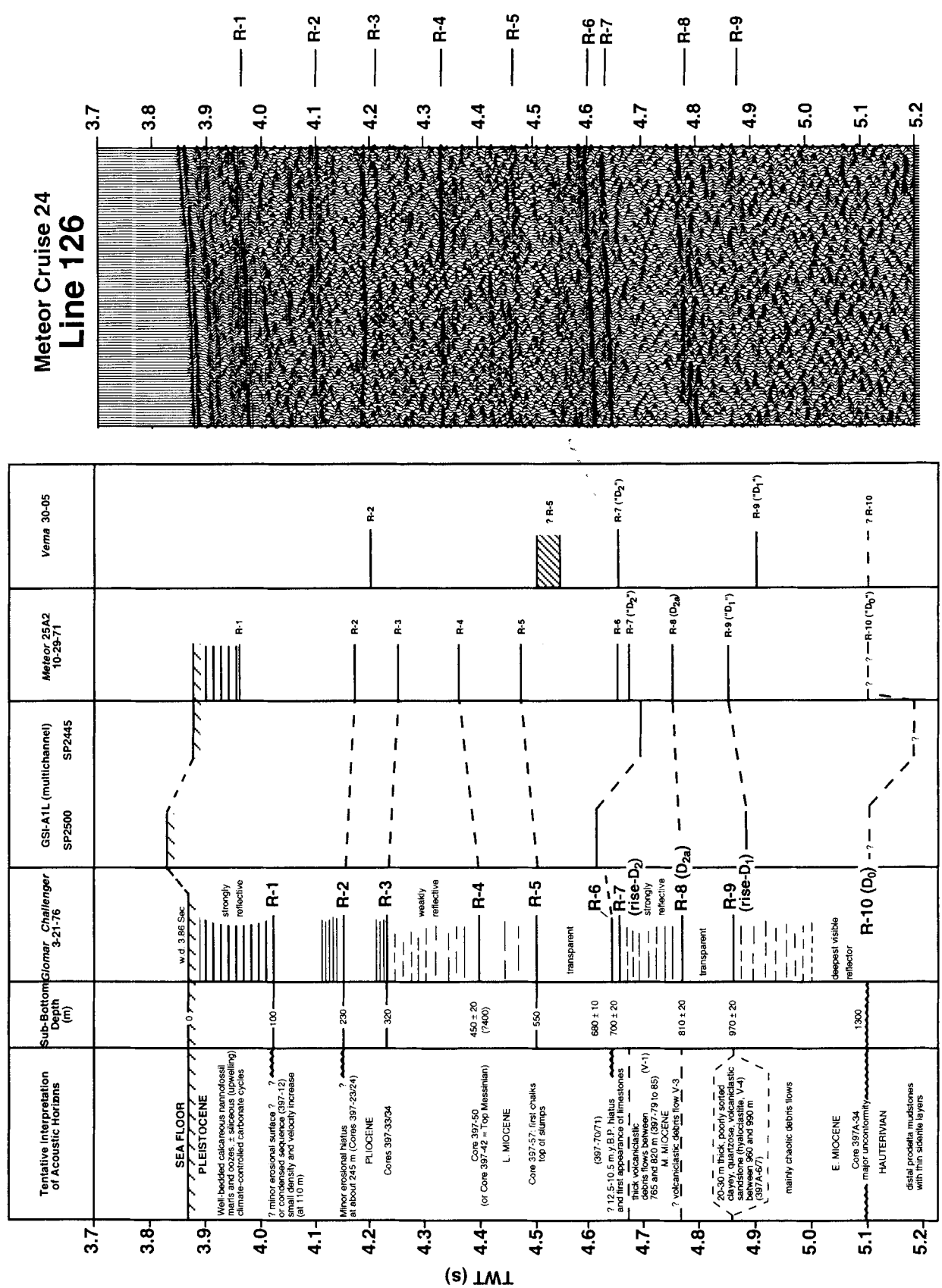

Figure 10. Correlation of DSDP Site 397 (adapted from von Rad *et al.* 1979) and the corresponding part of the time-migrated seismic line 126.

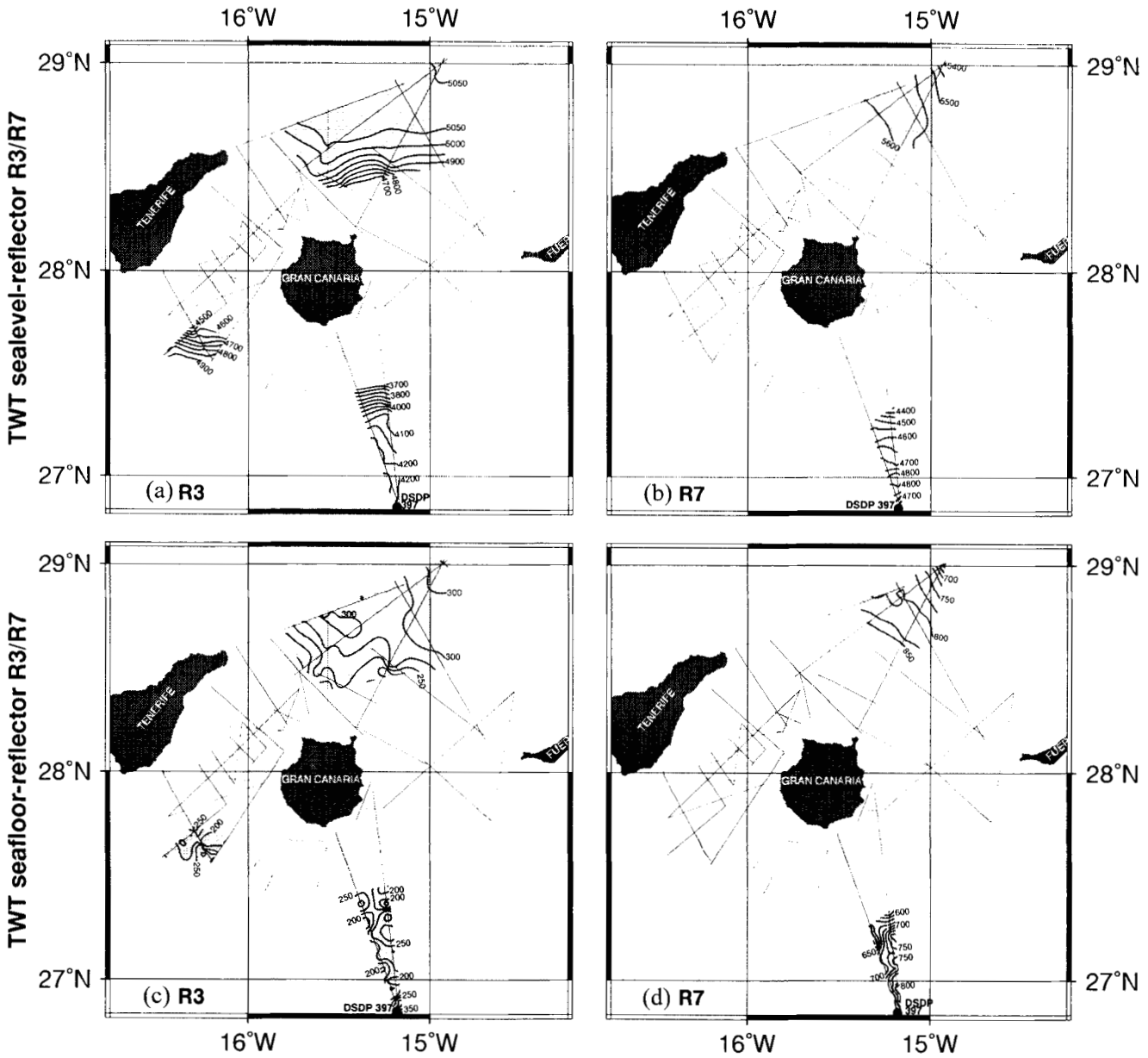

Figure 11. Correlation of the seismic reflectors R3 and R7. (a) Depth of reflector R3 below sea-level, measured in ms TWT. (b) Depth of reflector R7 below sea-level, measured in ms TWT. (c) Sediment coverage above reflector R3 (TWT in ms between the seafloor and R3). (d) Sediment coverage above reflector R7 (TWT in ms between the seafloor and R7).

reflectors in these areas, however, could not be directly correlated to the drill site due to the distribution of the seismic net and seismic chaotic facies between the islands, but were identified from their reflection pattern. In Fig. 11 this reflection band, which is interpreted as representing R3, is shown, together with reflector R7.

Reflector R7 was mapped in the more distal regions of Gran Canaria only, whereas the mapping of R3 is possible in more proximal regions. The depth of R3 and R7 below sea-level (Figs 11a and b) is greater in the north than in the south, as might be expected from the lower, eastward-decreasing water depths adjacent to the continental slope in the south.

The depth contour lines of R7 and R3 are fairly smooth, both in the north and the south (Figs 11a and b); there is, however, a remarkable difference between these areas in smoothness of the isopach lines (Figs 11c and d). In the northern basin the isopachs are much smoother than the small-scale thickness variations in the south. We interpret this as being due to the additional sediment supply in the southern basin derived from the continental slope (mainly by mass-wasting events), while the northern basin is protected from the African slope by the two eastern Canary Islands of Fuerteventura and Lanzarote. The influence of the nearby continental margin is illustrated on profile 126 (Fig. 12), where reflection patterns show a strong contrast between the well-stratified sediments of the northern basin (see e.g. profile 203 in Fig. 13a) and the reflectors in the south, which show more complex structures, are less continuous, and—most importantly—terminate frequently, indicating that a high amount of sediment was deposited during mass-wasting events, such as

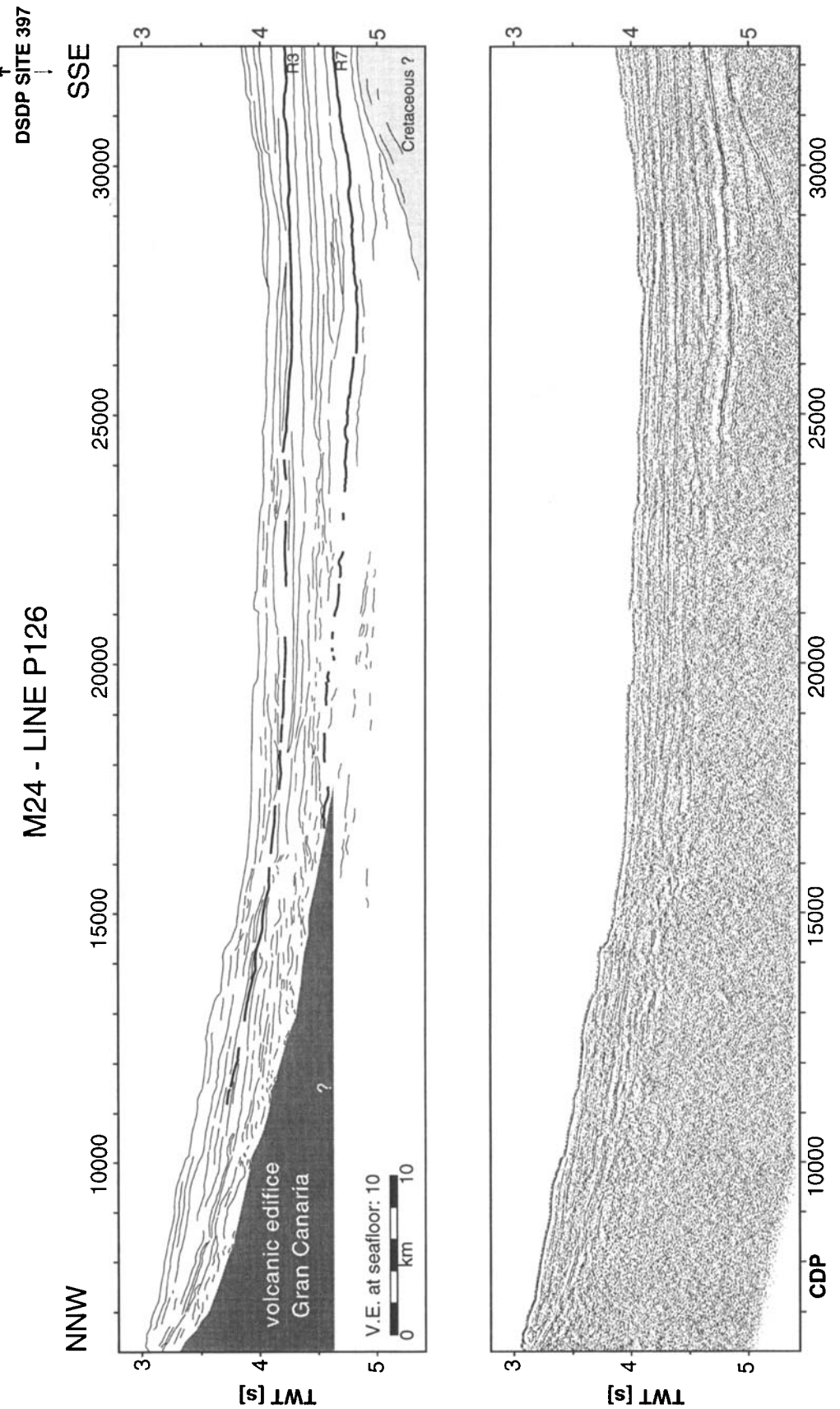

Figure 12. Southern part of time-migrated seismic line 126 and line drawing.

slumps and debris flows. Several periods of intense slumping have been detected accordingly at DSDP Site 397 (von Rad *et al.* 1979).

In the northern basin, reflector R7 dips gently towards the south-west (Fig. 11b). On closer inspection of profile 203 (Fig. 13a), such a dip of roughly 0.5° towards Gran Canaria is seen for all reflectors below R7 (i.e. below *ca.* 5.5 s TWT), whereas overlying reflectors are almost horizontal with onlap terminations against R7. The dip of the deep reflectors was probably caused by the response of the lithosphere to loading during the shield-building phase of Gran Canaria. At around 14 Ma the growth rate of the island decreased (Fig. 2). In general, the decrease of the subsidence related to loading postdates the loading event by some 0.5 to 1 Ma (Bodine, Steckler & Watts 1981). This is in good agreement with the age difference of reflector R7 (*ca.* 13.3 Ma), which marks the boundary between the dipping and the horizontal reflectors, and the end of the main shield-building phase. Continuing sedimentation gradually levelled out the dip, and the subsequent reflectors were deposited horizontally. The trend of the seismic data is also seen in the free-air gravity along profile 203 (Fig. 13a), where the values decrease as the infill of younger and less-dense sediment increases towards SSW. The depth of reflector R3 decreases towards the islands according

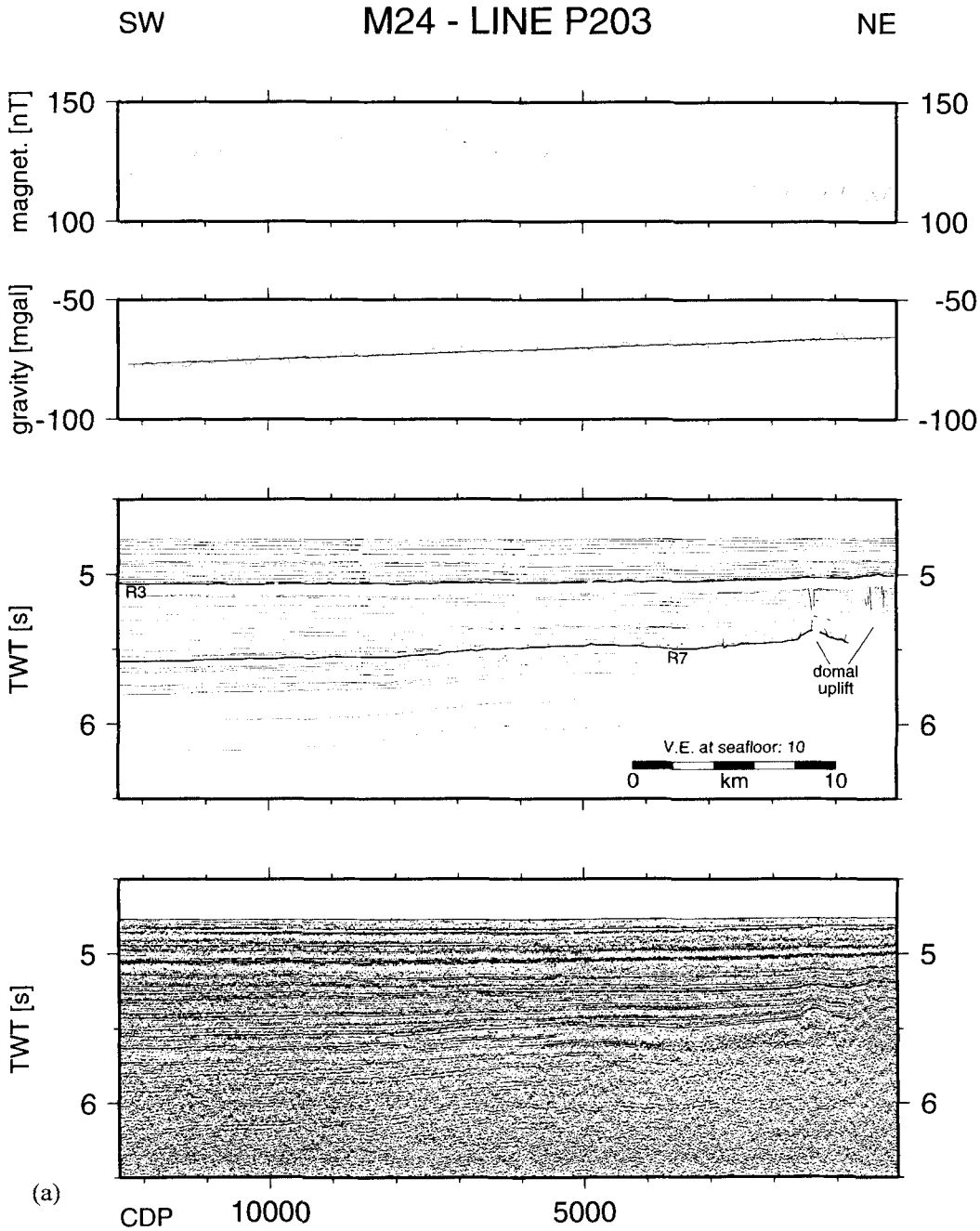

Figure 13. (a) Time-migrated seismic line 203 with line drawing, free-air gravity with best linear fit, and magnetic anomaly. The gravity and magnetic data were provided by G. A. Dehghani. (b) Simple magnetic model illustrating the theoretical influence of a magmatic intrusion at the location of the seismically defined domal uplift on profile 203. Depth converted from seismic time section.

to the morphology of the volcanic flank (Fig. 11b). One remarkable exception to this regular geometry is an uplift near the north-eastern limit of our survey area. This domal uplift is visible at the north-eastern ends of the seismic sections of lines 203 (Fig. 13a) and 202. All reflectors up to some 50 ms above R3 are updomed, and several fault systems are related to this structure, implying that the updoming had finished by late Pliocene. Three processes are conceivable as a cause for the updoming: (1) magmatic intrusion; (2) salt diapirism; or (3) mud diapirism of Early Cretaceous mud, as suggested in Fig. 12 of von Rad & Wissmann (1982). Gravity values would be expected to be reduced for a salt or mud body and increased for a magmatic intrusion. Since no significant deviation from the regional gravity trend is observed (Fig. 13a), a decision cannot be made based on gravity. Gravity modelling for such a deep and small domal uplift shows that the anomaly would not exceed a few mgal, which is close to the error or noise level of the gravity data. In the magnetics there is no anomaly visible either (Fig. 13a). In case of a magmatic body, the induced anomaly would probably have been a major feature in the magnetic field, as demonstrated by the simple model in Fig. 13(b). This implies a non-magmatic origin, i.e. either mud or salt diapirism. So far, no salt west of Fuerteventura and Lanzarote is known, but to the east, a zone of salt diapirism was mapped by Wissmann (1979) and Hinz, Dostmann & Fritsch (1982). The seaward limit of this diapir zone roughly corresponds with the eastward extension of the submarine shields of the two islands (Wissmann 1979). A more westward extension of the Jurassic salt zone would, however, have been masked seismically by the younger volcanic islands forming the acoustic basement. Therefore, we cannot exclude the possibility that the observed uplift structure close to the western limit of the submarine shield of Fuerteventura is caused by remnants of the Jurassic salt.

In contrast to salt domes, only a few examples of unambiguously proven mud diapirs are known offshore. They are located mostly at accretionary complexes (Henry *et al.* 1990; Camerlenghi *et al.* 1992). Brown (1990) described the important role of methane as the driving force for the intrusive process, pointing out that only a few per cent of pore space filled by free methane results in an increase of porosity and a decrease in density, which could then cause the necessary buoyancy.

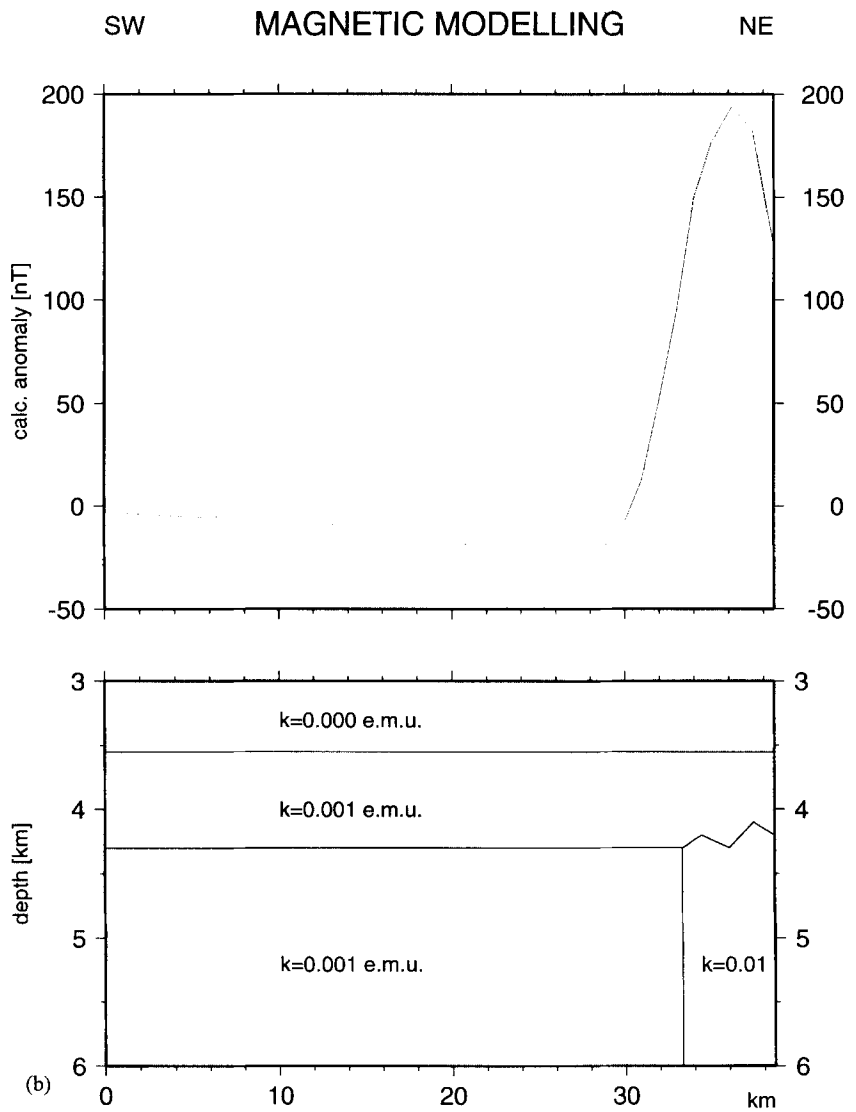

Figure 13. (*Continued.*)

The methane concentration in gas pockets found at DSDP Site 397 varied between 1 and 83 per cent (Whelan 1979). Hence, a mud origin of the uplift structure is also possible.

Closer to the island the correlation of the reflectors becomes more difficult, as deposition is characterized more and more by the flank facies, with its chaotic reflection pattern. In the case of reflector R3, no correlation closer than 28 km to Gran Canaria is possible. Even though the sediment thickness down to reflectors R3 and R7 is in general larger in the north than in the south (Figs 11c and d), a comparison of sedimentation rates between the northern and southern apron of Gran Canaria should be treated with caution, since the region mapped between profiles 126 and 127 in the south is, in contrast to the north, located at a continental rise, providing several additional mechanisms complicating regular sedimentation. Nevertheless, high-resolution reflection-seismic mapping of a dense profile net around Gran Canaria has provided detailed new information on the volcanic evolution of the central Canary Islands of Gran Canaria and Tenerife.

ACKNOWLEDGMENTS

This work was supported by the Deutsche Forschungsgemeinschaft (DFG-Schm250-54), the Bundesministerium für Forschung und Technologie (BMFT) and the EU (EPOCH, EVSV-CT93-0283). We acknowledge the first stage of reflection-seismic processing by S. B. Marstal at the University of Aarhus, Denmark. We are also grateful to G. A. Dehghani for placing gravity and magnetic data at our disposal, and to Captain Kull and his crew of RV METEOR. We appreciate valuable comments and suggestions to an early form of the manuscript by G. Wissmann.

REFERENCES

Ancochea, E., Fúster, J.M., Ibarrola, E., Cendrero, A., Coello, J., Hernán, F., Cantagrel, J.M. & Jamond, C., 1990. Volcanic evolution of the island of Tenerife (Canary Islands) in the light of new K-Ar data, *J. Volc. Geotherm. Res.*, **44,** 231–249.

Arthur, M.A., von Rad, U., Cornford, C., McCoy, F.W. & Sarnthein, M., 1979. Evolution and sedimentary history of the Cape Bojador continental margin, Northwestern Africa, in *Init. Rep. Deep Sea Drill. Proj.*, **47,** pp. 773–816, eds von Rad, U., Ryan, W.B.F. *et al.*, US Government Printing Office, Washington, DC.

Bodine, J.M., Steckler, M.S. & Watts, A.B., 1981. Observations of flexure and the rheology of the oceanic lithosphere, *J. geophys. Res.*, **86,** 3695–3707.

British Oceanographic Data Centre, 1994. *General bathymetric chart of the oceans (GEBCO),* 5th edn, Bidstone Observatory, Birkenhead, Merseyside, UK.

Brown, K.M., 1990. The nature and hydrogeologic significance of mud diapirs and diatremes for accretionary systems, *J. geophys. Res.*, **95,** 8969–8982.

Camerlenghi, A., Cita, M.B., Hieke, W. & Ricchiuto, T., 1992. Geological evidence for mud diapirism on the Mediterranean Ridge accretionary complex, *Earth planet. Sci. Lett.*, **109,** 493–504.

Coello, J., Cantagrel, J.-M., Hernán, F., Fúster, J.-M., Ibarrola, E., Ancochea, E., Casquet, C., Jamond, C., Díaz de Téran, J.-R. & Cendrero, A., 1992. Evolution of the eastern volcanic ridge of the Canary Islands based on new K-Ar data, *J. Volc. Geotherm. Res.*, **53,** 251–274.

Dañobeitia, J.J., Canales, J.P. & Dehghani, G.A., 1994. An estimation of the elastic thickness of the lithosphere in the Canary Archipelago using admittance function, *Geophys. Res. Lett.*, **21,** 2649–2652.

Geisslinger, A., 1993. Prozessing und Interpretation reflexionsseismischer Profile aus dem Bereich der Kanarischen Inseln, *Diplomarbeit,* Institut für Geophysik, Universität Hamburg.

Henry, P., Le Pichon, X., Lallemant, S., Foucher, J.-P., Westbrook, G. & Hobart, M., 1990. Mud volcano field seaward of the Barbados accretionary complex: a deep-towed side scan sonar survey, *J. geophys. Res.*, **95,** 8917–8929.

Hinz, K., Dostmann, H. & Fritsch, F., 1982. The continental margin of Morocco: seismic sequences, structural elements and geological development, in *Geology of the Northwest African continental margin,* pp. 34–60, eds von Rad, U., Hinz, K., Sarnthein, M., Seibold, E., Springer-Verlag, Heidelberg, Germany.

Hirschleber, H.B., Dañobeitia, J.J., Dehghani, G.A., Gallart, J., von Haugwitz, W., Herber, R., Radomski, S. & Schnaubelt, M., 1992. Geophysical investigations southwest of Gran Canaria (Canary Islands), *Oc.–Cont. Bound. Newslett.*, **1,** 33–39.

Hoernle, K.A. & Schmincke, H.-U., 1993a. The petrology of the tholeiites through melilite nephelinites on Gran Canaria, Canary Islands: crystal fractionation, accumulation, and depths of melting, *J. Petrol.*, **34,** 573–597.

Hoernle, K.A. & Schmincke, H.-U., 1993b. The role of partial melting in the 15-Ma geochemical evolution of Gran Canaria: A blob model for the Canary Hot Spot, *J. Petrol.*, **34,** 599–627.

Hoernle, K.A., Tilton, G. & Schmincke, H.-U., 1991. Sr-Nd-Pb isotopic evolution of Gran Canaria: evidence for shallow enriched mantle beneath the Canary Islands, *Earth planet. Sci. Lett.*, **106,** 44–63.

Hunter, P.M., Searle, R.C. & Laughton, A.S., 1980. *Bathymetry of the northeast Atlantic—sheet 5. Continental margin off northwest Africa,* Institute of Oceanographic Sciences, NERC, UK.

McDougall, I. & Schmincke, H.-U., 1976. Geochronology of Gran Canaria, Canary Islands: Age of shield building volcanism and other magmatic phases, *Bull. Volcanol.*, **40,** 57–77.

Menard, H.W., 1956. Archipelagic aprons, *Am. Assoc. Petrol. Geol. Bull.*, **40,** 2195–2210.

Menard, H.W., 1964. *Marine geology of the Pacific,* McGraw-Hill, New York, NY.

National Geophysical Data Center, 1993. *Database for marine geophysical data,* NOAA E/GC4, Dept. 940, Boulder, CO.

ODP Leg 157 Shipboard Scientific Party, 1995. Gran Canaria volcanic apron and Madeira Abyssal Plain drilled, *EOS, Trans. Am. geophys. Un.*, **76,** 393–395.

Ranke, U., von Rad, U. & Wissmann, G., 1982. Stratigraphy, facies and tectonic development of the on- and offshore Aaiun-Tarfaya Basin—a review, in *Geology of the Northwest African continental margin,* pp. 86–105, eds von Rad, U., Hinz, K., Sarnthein, M., Seibold, E., Springer Verlag, Heidelberg, Germany.

Rothe, P. & Koch, R., 1978. Miocene volcanic glass from DSDP Sites 368, 369, and 370, in *Init. Rep. Deep Sea Drill. Proj.*, **41,** pp. 1061–1064, eds Lancelot, Y., Seibold, E. *et al.* US Government Printing Office, Washington, DC.

Schmincke, H.-U., 1976. Geology of the Canary Islands, in *Biogeography and Ecology in the Canary Islands,* pp. 67–184, eds Kunkel, G. & Junk, W., The Hague, The Netherlands.

Schmincke, H.-U., 1982. Volcanic and chemical evolution of the Canary Islands, in *Geology of the Northwest African continental margin,* pp. 273–306, eds von Rad, U., Hinz, K., Sarnthein, M., Seibold, E., Springer-Verlag, Heidelberg, Germany.

Schmincke, H.-U., 1994. *Geological field guide of Gran Canaria, parts 1 & 2,* 7th edn, Pluto Press, Kiel, Germany.

Schmincke, H.-U. & Rihm, R., 1994. Ozeanvulkan 1993—Cruise No. 24, 15 April–9 May 1993, *METEOR-Berichte,* **94–2,** Universität Hamburg, Germany.

Schmincke, H.-U. & von Rad, U., 1979. Neogene evolution of Canary Island volcanism inferred from ash layers and volcaniclastic sandstones of DSDP Site 397 (Leg 47A), in *Init. Rep. Deep Sea Drill. Proj.*, **47,** pp. 703–725, eds von Rad, U. *et al.*, US Government Printing Office, Washington, DC.

Seibold, E. & Hinz, K., 1976. German cruises to the continental margin of North West Africa in 1975: general reports and preliminary

results from VALDIVIA-10 and METEOR-39, *METEOR-Forsch.-Ergebnisse,* Reihe C, **25,** 47–89.

Thywissen, K. & Wong, H.K., 1993. *Teilabschlußbericht zum Projekt reflexionsseismische Untersuchungen im Bereich der Kanaren—METEOR-Fahrt 16/4—Presite-Survey im Rahmen von VICAP im Schwerpunkt 'Auswertung der METEOR-Expeditionen',* Deutsche Forschungsgemeinschaft, Bonn, Germany.

Uchupi, E., Emery, K.O., Bowin, C.O. & Phillips, J.D., 1976. Continental margin off Western Africa: Senegal to Portugal, *Am. Assoc. Petrol. Geol. Bull.,* **60,** 809–878.

von Rad, U. *et al.,* 1979. *Init. Rep. Deep Sea Drill. Proj.,* **47,** US Government Printing Office, Washington, DC.

von Rad, U. & Wissmann, G., 1982. Cretaceous-Cenozoic history of the West Saharan continental margin (NW Africa): development, destruction and gravitational sedimentation, in *Geology of the Northwest African continental margin,* pp. 106–131, eds von Rad, U., Hinz, K., Sarnthein, M., Seibold, E., Springer-Verlag, Heidelberg, Germany.

Wefer, G., Schulz, H.D., Schott, F. & Hirschleber, H.B., 1992. Atlantik 91–Expedition, Reise Nr. 16, 27. März–8. Juli 1991, *METEOR-Berichte,* **92–2,** Universität Hamburg, Germany.

Whelan, J.K., 1979. C_1 to C_7 hydrocarbons from IPOD Holes 397 and 397A, in *Init. Rep. Deep Sea Drill. Proj.,* **47,** pp. 531–539, eds von Rad, U. *et al.,* US Government Printing Office, Washington, DC.

Wissmann, G., 1979. Cape Bojador Slope, an example for potential pitfalls in seismic interpretation without the information of outer margin drilling, in *Init. Rep. Deep Sea Drill. Proj.,* **47,** pp. 491–499, eds von Rad, U. *et al.,* US Government Printing Office, Washington, DC.

Ye, S., Rihm, R., Canales, J.P., Dañobeitia, J.J. & Gallart, J., 1995. Crustal transect through volcanic island Gran Canaria, *Ann. Geophys.,* Suppl. 1, **13,** C128.